Key Engineering Materials *Online: 2013-07-15*
ISSN: 1662-9795, Vols. 562-565, pp 1346-1352
doi:10.4028/www.scientific.net/KEM.562-565.1346

Smart Structural Health Monitoring Based on Detecting Picometer-scale Wavelength Shift of Fiber Bragg Grating

Bai Junjie[1,2,a], Li Jianxing[2], Zhang Jun[3], Zhang Xiaoyun[1], Wang Le[4], Wu Ying [1,b]

[1]College of Electrical and Information Engineering, Chongqing University of Science and Technology, Chongqing 401331, China

[2]College of Instrument Science and Engineering, Southeast University, Nanjing 210096, China

[3]Southeast Oil and Gas Field Mining Services Division, 610051, China

[4]Chongqing University of Posts and Telecommunications, Chongqing, 400065, China

[a]junjie_7654@163.com, [b]yingwucindy@yahoo.com.cn (corresponding author)

Keywords: Smart civil structure; Structural health monitoring; Fiber Bragg grating; Wavelength demodulation; Fiber comb filter

Abstract. The real-time monitoring technologies of smart civil structure based on detecting picometer-scale wavelength shift of fiber Bragg grating (FBG), including the wavelength demodulation technology of FBG, are researched extensively at home and abroad. In the paper, using the technologies of wavelength division multiplex (WDM) and time division multiplex (TDM), fiber Bragg grating (FBG) sensor network was built for monitoring smart structure health condition. Based on SOPC (System on Programmable Chip) technology and fiber comb filter, a high-speed and high-precision wavelength demodulation scheme of FBG sensor network was proposed. The optical system and hardware circuit for demodulation system were designed specifically. To improve the accuracy of demodulation system of FBG, a constant temperature channel of the demodulation system connected with a fiber comb filter, which offered reference points to calibrate the Bragg grating center wavelength. Based on 32-bit soft-core processor Nois Ⅱ, the embedded system collected and processed the photoelectric signal voltage transformed to rectangular voltage pulse. The upper computer displayed dynamically the FBG wavelength demodulation process and calibrated the Bragg grating center wavelength. The experiments of FBG wavelength demodulation and health monitoring of smart structural embedded fiber Bragg gratings were done. Experimental results show that, the FBG wavelength demodulation method can be used to demodulate the FBG wavelength with high speed and high precision (± 2 pm), which can be used extensively in large-scale multipoint monitor engineering, and the strains of the smart structure can be measured accurately.

Intorduction

Since Morey firstly reported the fiber grating sensing technology in1989, this technology has received extensive attention and developed rapidly [1]. In 1993, using 16 Fiber Bragg Grating sensors, the structure health monitoring of Beddington Trail Bridge was realized in Canada [2]. In recent years, fiber Bragg grating sensing technology, which has become a research focus at home and abroad, is widely used in structure health monitoring of large civil engineering [3-5].

For the FBG sensors embedded in civil structure construct sensor network, the civil structure constructs become smart structures with some abilities, such as self-awareness, self-analysis, self-calculation, self-reasoning, self-control, and so on. Since Prohaska of Rutger University first embedded FBG sensors into the concrete structure to measure strains in1992, domestic and foreign scholars have done a lot of work on smart civil structures and intelligent monitoring technologies [6-9].

However, how to measure speed and precisely the picometer-level resonant wavelength shift of FBG is the key to monitor the health of smart structure in real time. Based on embedded processors, such as MCU, DSP, and ARM, some wavelength demodulation systems were designed, and the unknown

FBG wavelength was calibrated through the standard wavelengths of fiber Bragg gratings placed in a constant channel [10-12]. The speed and precision of the wavelength demodulation need to be further improved.

In the paper, based on Altera's 32-bit soft-core processor Nios Ⅱ and fiber comb filter, a new wavelength demodulation and calibration system for FBG sensing network was developed, which is high-speed and high-precision. The structural health monitoring experiment of the smart reinforced concrete structure with FBG sensors has been done.

Sensing Principle of FBG

FBG can play a role of mirror, but it must satisfy the reflection condition, Bragg condition:

$$\lambda_B = 2n_{eff}\Lambda \tag{1}$$

where λ_B, n_{eff}, and Λ are the center wavelength of FBG's reflected light, the effective refractive index of fiber core area, and the grating period, respectively.

According to the Bragg condition, it can be concluded that:

$$\Delta\lambda_B = 2\Delta n_{eff}\Lambda + 2n_{eff}\Delta\lambda \tag{2}$$

According to elasticity mechanics, the changes of FBG center wavelength, $\Delta\lambda_B$ can be expressed as:

$$\Delta\lambda_B = 2n_{eff}\Lambda\{\{1-\frac{n^2_{eff}}{2}[p_{12}-\mu(p_{11}+p_{12})]\}\varepsilon_a + (\alpha_s+\xi_s)\Delta T\} \tag{3}$$

where ε_a, μ, α_s, ξ_s, and ΔT are axial strain, Poisson's ratio of fiber material, coefficient of thermal expansion of fiber material, thermo-optic parameters of fiber material, and temperature change of FBG, respectively; p_{11} and p_{12} are photoelastic coefficients of the fiber material.

Take into account the parameters of SiGe optical fiber, $\Delta\lambda_B$ can be represented as the following equation,

$$\Delta\lambda_B = 0.78\lambda_B\varepsilon_a + 6.67\times10^{-6}\lambda_B\Delta T \tag{4}$$

The expression (4) shows that, if only consider the change of temperature or stress, there is a linear relationship between $\Delta\lambda_B$ and ε_a, and there is a linear relationship between $\Delta\lambda_B$ and ΔT. In the light of the expression (4), it also can be seen that FBG is sensitive to temperature and strain at the same time. Based on the cross sensitive characteristic of FBG, there are many effective ways to measure simultaneously temperature and strain.

Wavelength Demodulation of FBG Sensor Network

FBG Wavelength Demodulation System

It is difficult to demodulate FBG wavelength and the cost of wavelength demodulation is high. To achieve high-precision demodulation of FBG wavelength, it involves two aspects. First, because the spectral width of Bragg wavelength is less than 0.3 nm, to improve the measurement accuracy of the amount of Bragg wavelength shift, the peak point of the FBG reflection spectrum must be identified and the movement of peak point must be tracked accurately. Second, the amount of peak-point movement measured accurately must be translated into electrical signals for measurement purpose.

Using a tunable Fabry–Perot filter (TFPF), fiber comb filter, and an optical switch to set up the optical path, the wavelength demodulation of FBG sensing network with three channels was achieved, which can monitor nearly one hundred of the external signals with high speed and high precision. The wavelength demodulation scheme is shown in Fig. 1. First, the broadband light source (SLED, Super LED) having a bandwidth of 50 nm centered at 1310 nm or 1550 nm irradiated an optical switch through 3 db directional coupler. The optical switch was controlled by program and the four channels were opened in turn. In the three optical channels connected with fiber Bragg gratings, a series of optical narrowband pulses were reflected, and another series of narrowband optical pluses

transmit from the fiber comb filter placed inside the constant temperature channel. Then, the optical narrowband pluses of each channel transmitted into the TFPF in turn. The TFTP was controlled by triangle-wave scanning voltage. There is a linear relationship between the center wavelength transmitting form the TFTP and the scanning voltage. In the same scanning cycle, the narrowband light pulses with different center wavelengths passed through TFPT at different moment. These optical narrowband pluses can detect the Bragg wavelengths of FBG sensors. The different Bragg wavelengths made different peak points and these peak points were detected by a photo diode in turn. The voltage signal detected by photo-diodes is filtered and amplified and finally shaped into rectangular impulse which was acquired and processed by the embedded system based on 32-bit soft-core processor Nois Ⅱ. The Bragg wavelength shifts of FBG sensors were observed and plotted via demodulation program of upper computer. The switching frequency of optical switch was kept pace with the scanning-voltage frequency of TFPF.

The spectral bandwidth of SLED (Supper light-emitting diode) is 40 to 50 nm, and the bandwidth of the reflection spectrum of FBG is 0.07 to 0.6 nm. When detecting external signals, the center wavelength of FBG drifts 1 to 2 nm. In order to ensure that the reflection spectrums of FBG sensors do not overlap, no more than 30 FBG sensors can be connected in a same fiber. A large-scale project often require hundreds of different locations to be monitor simultaneously, which requires the development of distributed multi-channel FBG sensor system with high speed and precision. As is shown in Fig. 1, the wavelength demodulation system can be used extensively in large-scale multipoint monitor engineering.

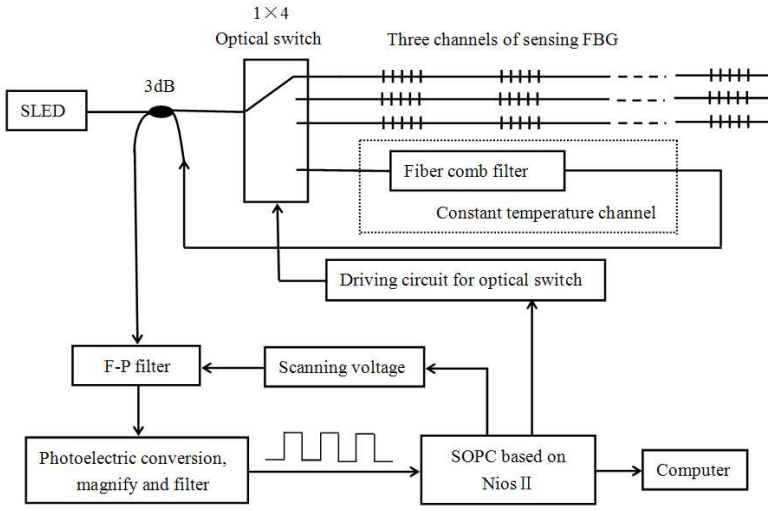

Fig. 1 Wavelength demodulation system for FBG sensor network

SOPC Module Based on NIOS Ⅱ

The soft-core Nios Ⅱ embedded processor was introduced by Altera Corporation in 2004. Using Altera's MegaWizard interface, the designer can map a system and configure memory and peripherals. For example, the designer can choose from a variety of widths and speeds of memory as well as peripheral types. Furthermore, the Nios Ⅱ embedded processor core can be extended in three ways, including adding conventional memory-mapped peripherals on-chip, mapping readable/writeable devices into the processor's register file, and adding user-designed function blocks directly into the processor's arithmetic logical unit.

As shown in Fig. 1, the SOPC module based on Nios Ⅱ is the core-function module, which realized data acquisition and processing, generating and controlling triangle wave scanning voltage, controlling optical switch, controlling some peripherals interfaces, and so on. Based on Altera SOPC builder tool, SOPC system is customized, and System frequency is 33 MH. The system hardware design block diagram is shown in Fig. 2. PIO is the parallel input/output controller. PIO_0 and PIO_1 were configured as level-trigger interfaces, which result in external interrupts when signal rising edges are detected. PIO_2 was configured as the parallel input/output interface. The SOPC module

acquired and processed voltage signal shaped into rectangular impulse, which determined relative moment when the central location of rectangular impulse occurred in a scan-voltage cycle shown in Fig. 1.

The method of determining relative moment when the central location of rectangular impulse occurred in a scan-voltage cycle is described as follows. The high-frequency count pulse was inputted into the counter embedded in the FPGA. The photoelectric voltage signals shaped into rectangular impulse were inputted into the PIO_2. The triangle-wave scanning voltage of Fig. 1 was converted to square wave signal. The square wave was inputted into PIO_0 and the reverse signal of square wave was inputted into PIO_1. When the rising edge of square wave appeared, the counter started counting. When the falling edge of square wave signal appeared, the counter was zeroed. Based on query modes, the values of the counter were stored when the rising or falling edge of rectangular impulse inputted into PIO_2. When the rising edge of rectangular impulse appeared, the value of the counter was N_1. When the falling edge of rectangular impulse appears, the value of the counter was N_2. Then, the count pulse number N, which corresponds with the central location of the rectangular impulse, was $(N_1+N_2)/2$ and was transmitted to the computer via the RS232 or USB interface.

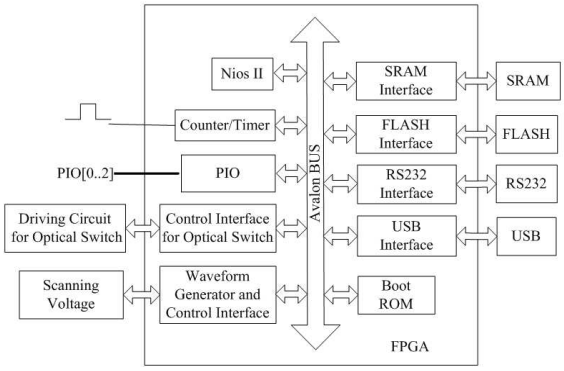

Fig. 2 SOPC module based on Nios Ⅱ

There is linear relation between the count pulse number N and the Bragg wavelength λ, which can be used to calculate the real-time Bragg wavelength of FBG [13].

Wavelength Calibration Experiment

Experimental Methods. Based on the above demodulation scheme, the multi-channel wavelength demodulator was developed, and the wavelength calibration experiments were done. Fig.3 is the experiment system structure diagram. One channel of the wavelength demodulator connected three fiber Bragg gratings, and a fiber comb filter was connected with another channel which was kept in constant temperature status. The wavelength demodulator transmitted central locations of the rectangular impulses to PC via RS232 interface. According to the relation between central location N_i of the rectangular impulse and center wavelength λ_i of FBG (or center wavelength λ_i of narrowband light impulse outputted from fiber comb filter), the unknown FBG wavelength can be calibrated. In order to verify wavelength demodulation precision, fiber Bragg gratings were placed in a thermostat to avoid temperature change.

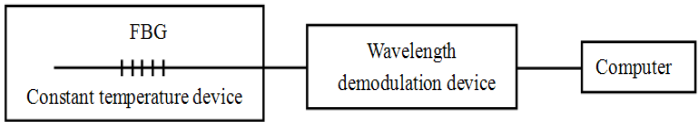

Fig. 3 The structural diagram of experimental system for calibration

Experimental Results. The transmission light center wavelengths of the fiber comb filter (λ_i, i=1-15) were measured by a high-precision spectrometer, and were distributed in 1294.078-1309.907 nm. The wavelength demodulator detected central locations (N_i, i=1-15) of the rectangular impulse signal voltage corresponding λ_i. There is an almost linear relationship between λ_i and N_i. N_i and λ_i composed reference points, (N_i, λ_i), for calibration. According to different interpolation methods, the

center wavelengths of fiber Bragg gratings were calibrated. Table 1 shows that, wavelength calibration precision based on spline interpolation method is ± 2 pm but the algorithm is relatively complicated, and wavelength calibration precision based on piecewise linear interpolation method is ± 4 pm but the algorithm is relatively simple.

Table 1 Results of calibration experiment

Wavelength measured by spectrometer (nm)	Piecewise linear interpolation wavelength (nm)	Piecewise linear interpolation wavelength error (pm)	Spline interpolation wavelength (nm)	Spline interpolation wavelength error (pm)
1298.447	1298.4435	3.5	1298.4453	1.7
1305.033	1305.0316	1.4	1305.0327	0.3
1307.653	1307.6561	3.1	1307.6542	1.2

Experiment of intelligent civil structure Strain Monitoring

Experimental Procedure

In order to measure the internal strain of concrete structure, the fiber Bragg gratings produced by the mask in the same batch was used in the experiment, and the wavelength demodulation was achieve by self-developed Bragg wavelength demodulation platform. Before pouring the concrete, the strain sensitivity coefficient and the temperature sensitivity coefficient were measured respectively by the tensile test machine and the water bath method. Then, five FBG sensors were pasted on the reinforced steel surface. The installation locations of FBG sensors are shown in Fig. 4. Concrete beam length is 2 m, width is 0.18 m, and height is 0.25 m. A standard single-mode optical fiber acted as optical signal transmission. By way of welding, five FBG sensors were welded in an optical fiber. Owing to lower strength, the weld points were protected by heat-shrinkable tubes. In the construction process, in order to resist the impact of concrete pouring and prevent the FBF sensors to be damaged, the FBG sensors were coated by epoxy resin. The whole optical fiber was protected by a casing with 15 mm diameter, which was fixed on the cross-section reinforced steel.

After the maintenance period, concrete structure achieved the desired strength and Four-point bending load experiment of the beam was done. Before the experiment, the surface of the beam with the FBG sensors was also pasted resistance strain gauges at the same horizontal position.

During the experiment, according to different load levels controlled by force sensor, hydraulic jack applied load on the reinforced concrete beam shown in Fig. 4. The strains of the beam were measured respectively by FBG sensors and resistance strain gauges and the results are basically consistent. The strain curves of reinforced concrete beam at the midpoint are shown in Fig. 5.

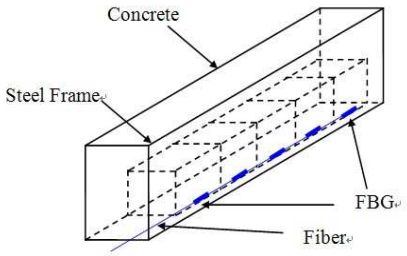

Fig. 4 Reinforced concrete beams with FBG sensors

Experimental Results

During strain monitoring experiment of the reinforce concrete beam, the impact of temperature on the strain measurement was ignored due to temperature fluctuations of only 0.2 ℃ in the laboratory. The results show that the FBG sensors embodied in the reinforced concrete have good sensing properties, such as fast response to strain, stable performance, and so on.

The strain curves of FBG and resistance strain gauge are in good agreement, which shows the beam is within the scope of elastic deformation, no relative slip between reinforced steel and concrete appear, and the FBG sensors pasted in the reinforcing steel can detect the internal strains of the beam.

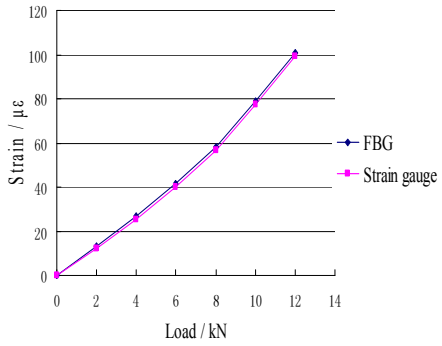

Fig. 5 Strain curves of reinforced concrete beam

Acknowledgements

This work was supported in part by NSFC under Grant No. 60876088 and Grant No. 51105398, the Supporting Program for Excellent Talents of University in Chongqing, and Research Foundation of Chongqing University of Science & Technology (Grant No. CK2011Z09）

References

[1] G. Meltz, W. W. Morey, W. H. Glenn, Formation of Bragg gratings in optical fibers by a transverse holographic method, Optics Letters, 14 (1989) 823–826.

[2] R. C. Tennyson, A. A. Mufti, S. Rizkalla, Structural health monitoring of innovative bridges in Canada with fiber optic sensors, Smart Mater. Struct., 10 (2001) 560–573.

[3] Yue Lina , Huang Jun, Jiang Desheng, Application of Optical Fiber Sensing Technology in Strengthening Monitoring of Wuhan Second Yangtze River Bridge, JOURNAL OF WUHAN UNIVERSITY OF TECHNOLOGY, 31(2009) 10–12.

[4] Li Dongsheng, Deng Nianchun, Ou Jinping, Fiber Bragg Grating Sensor Monitoring Techniques and Health Diagnosis of Arch Bridge Suspenders, Journal of Optoelectronics · Laser, 18 (2007) 81–84.

[5] Li Dongsheng, Zhou Zhi, Ou Jinping, Development and sensing properties study of FRP–FBG smart stay cable for bridge health monitoring applications, Measurement, 44 (2011) 722–729.

[6] S. Lu, H. Xia, Strengthen and real-time monitoring of RC beam using intelligent CFRP with embedded FBG sensors, J. Construct. Build. Mater. , 21 (2007) 1839–1845.

[7] J.S. Leng, G.C. Mays and G.F. Fernando, Structural NDE of concrete structures using protected EFPI and FBG sensors, Sens. Actuators,126 (2006) 340–347.

[8] G. Kister, D. Winter, J. Leighton, Grattan and G.F. Fernando, Methodology and integrity monitoring of foundation concrete piles using Bragg grating optical fibre sensors, Eng. Struct. , 29 (2007) 2048–2055.

[9] A.C. Wong, P.A. Childs, R. Berndt, Simultaneous measurement of shrinkage and temperature of reactive powder concrete at early age using fiber Bragg grating sensors, Cem. Concr. Comp., 29 (2007) 490–497.

[10] Qiren Z. , Dongmei G. , Jing W. , A High Precise Sensing Demodulation Technology Based on Fiber-Grating Sensors and Single-Chip Microcomputer, Journal of Huaqiao University (Natural Science), 25 (2004) 254-257.

[11] Xiaozong D, Changsong W, Xianfeng G, Development of a Wavelength Demodulator for Fiber Bragg Grating Based on DSP, SEMICONDUCTOR OPTOELECTRONICS, 29 (2008)778-781.

[12] Guangxue Y. , Feng B. , Research on Fiber Bragg Grating seismic observation system based on ARM, WORLD EARTHQUAKE ENGINEERING, 27 (2011) 202-206.

[13] Bai Junjie, Wang Lixin, Ran Changyan, Demodulating and Calibrating for Fiber Bragg Grating Based on Fabry-Perot Filter, Transducer and Microsystem Technology, 25(2006) 10–12.